X-662-71-209
PREPRINT

NASA TM X- 65564

GAMMA RAY OBSERVATIONS OF THE GALACTIC CENTER AND SOME POSSIBLE POINT SOURCES

C. E. FICHTEL
R. C. HARTMAN
D. A. KNIFFEN
M. SOMMER

JUNE 1971

GSFC
GODDARD SPACE FLIGHT CENTER
GREENBELT, MARYLAND

GAMMA RAY OBSERVATIONS OF THE GALACTIC CENTER AND SOME POSSIBLE POINT SOURCES

C. E. Fichtel, R. C. Hartman, D. A. Kniffen, and M. Sommer*
NASA/Goddard Space Flight Center, Greenbelt, Md. 20771

ABSTRACT

A (.5 m by .5 m) digitized spark chamber gamma ray telescope was flown on three balloon flights to look at the galactic center region, Virgo, and the Crab. An excess flux above atmospheric background of over four standard deviations was found for gamma rays exceeding 100 MeV coming from the galactic center region, corresponding to a line intensity of $(2.0 \pm 0.6) \times 10^{-4}$ γ's$(cm^2 rad\ sec)$, but there was no statistically significant excess in the 50 to 100 MeV interval, with a 95% confidence limit for the ratio [J(50-100 MeV)/J(> 100 MeV)] being 0.50. As a result, there is only a 6% chance that Compton or synchrotron radiation from electrons with a power law spectrum having an exponent of 2.6 could make as much as a 50% contribution to the gamma radiation in this energy range. No positive evidence was found for radiation from any of the sources M 87, 3C273, and the Crab Nebula, and 95% confidence upper limits for the gamma ray flux from these objects were set at $1.0 \cdot 10^{-5}$, $1.0 \cdot 10^{-5}$, and $6 \cdot 10^{-5}/(cm^2 sec)$ respectively. The M-87 limit eliminates the possibility that the power law spectrum observed at X-ray energies extends unchanged to the high energy gamma ray region.

*NAS-NRC Postdoctoral Resident Research Associate. Present address: Max-Planck Institut für Extraterrestriche Physik, München, Germany.

I. INTRODUCTION

In spite of the considerable effort that has been extended during the last decade to detect high energy (> 20 MeV) celestial gamma rays, relatively few positive results have been obtained, although significant upper limits on the flux from several possible discrete sources have been set using data from balloon experiments. The most positive evidence for an extraterrestrial source of high-energy γ-rays has come from the counter telescope experiment of Clark, Garmire, and Kraushaar (1968) flown on OSO-III. These authors have presented convincing evidence for the detection of γ-radiation from the galactic plane, with the greatest intensity coming from the region of the galactic center.

Both in an attempt to measure the intensity and energy spectra of galactic γ-rays above 25 MeV from balloon altitudes and with the goal of developing a satellite-qualifiable γ-ray telescope, a large digitized spark-chamber γ-ray detector was built and flown on high-altitude balloons. This detector, whose active spark chamber area is about 2.5 x 10^3 cm^2, is about ten times the size of the original Goddard spark chamber first flown in 1966. Preliminary results from one of the flights with the larger telescope, which confirmed the existence of the galactic center radiation, were presented earlier (Kniffen and Fichtel, 1970). Here, the experiment will be described in more detail together with the final results from the balloon flights made thus far.

II. DESCRIPTION OF THE GAMMA-RAY TELESCOPE

A schematic diagram of the spark chamber gamma-ray telescope is shown in Fig. 1. The active parts of the detector are the 0.5 x 0.5 m

digitized spark chambers and the triggering counter system. The spark chamber stack is assembled from a total of thirty-two modules, eleven of them being placed above the central scintillator level. Each module consists of two orthogonal sets of 400 parallel wires forming two wire grids with 4 mm vertical spacing. Stainless steel plates of 0.03 radiation lengths thickness between the upper wire modules provide conversion of gamma-rays into pairs. Plates of 0.02 radiation lengths between the lower modules are used to obtain information on the energy of the individual positron and negatron from Coulomb scattering. Sparks will occur along the paths of the electrons when a high voltage pulse is applied to the wire grid shortly after detection of the electron pair by the counter telescope. The resultant spark current propagates along the orthogonal wires setting ferrite cores at the end of the wires. In this manner, x- and y- coordinates are obtained for each electron track at every module or z-level. The spark coordinates are described by a number of 16-bit words which are transmitted by telemetry to the ground station within a total time of about 0.3 seconds for an average event.

The spark chamber triggering logic is chosen to accept gamma-rays and to reject other events to a high degree. A coincidence signal is required from one of the nine charged-particle-telescopes. Each of these is formed by a 16.5 x 16.5 x 0.48 cm plastic scintillator and a 16.5 x 16.5 x 5 cm plexiglass Cerenkov counter. The spark chamber is triggered when a neutral particle is converted into one or more downward-moving relativistic charged particles actuating one or more of the nine charged-particle-telescopes. Primary charged particles are rejected by anti-coincidence signals produced in the surrounding scintillator dome. The

dome is a highly polished single-piece casting of plastic scintillator measuring 1.2 m inside diameter, 0.8 m in height, and 1.6 cm in thickness. It is viewed by 18 photomultiplier tubes spaced evenly around the lower edge.

A more detailed description of the 0.5 m by 0.5 m digitized spark chamber gamma ray telescope is given by Ross et al. (1969).

III. DATA REDUCTION AND ANALYSIS

Data including a variety of housekeeping parameters and information on which of the magnetic cores in the spark chamber have been set in each event are telemetered from the balloon gondola and recorded on magnetic tape together with time signals accurate to two milliseconds. The housekeeping information includes 3-axis magnetometer readings which together with time and balloon position provide the basis for determining the experiment aspect, individual counter and coincidence rates, experiment dead time, and engineering parameters such as temperatures, pressures, voltages, and currents.

The spark chamber data reduction includes identification of gamma ray events, estimation of the gamma-ray energy from the scattering of the electron pair in the steel plates, and determination of the celestial arrival direction, utilizing the magnetometer data to obtain the instrument orientation. The general approach and details for the calculation of the energy and arrival direction of individual gamma rays, have been described previously together with the method of determining flux values (Fichtel et al., 1969). Therefore, they will not be repeated here. In the interim, however, the computer programs have been developed to the extent that gamma ray identification and electron track recognition are

largely automatic, and the human interface time has been greatly reduced. A minimum interface for the purpose of verifying that the program is functioning properly is maintained.

The procedures for automatic recognition will now be summarized. The automatic analysis program rejects any event which:

1) has any set cores in the top deck (representing generally either a gamma ray which has converted in the pressure vessel shell under the anticoincidence dome or a charged particle missed by the anticoincidence system),
2) has a set core within two wires of the edge of any of the top ten modules (and therefore would usually correspond to a gamma ray which interacted in the spark chamber walls),
3) has less than 15 cores set in either orthogonal view (indicating no event, usually a false trigger).

The program then begins the search for gamma ray events by averaging groups of two or more adjacent set cores to obtain points which will represent the basis for the "picture" of the events in each of the two orthogonal views (x-z and y-z). The program then scans downward from the top of the spark chamber until it finds the occurrence of three decks containing points within a five-deck span. Within those three decks, it forms all possible triads with one point in each deck. For each triad it forms the second difference $\beta_i = X_i - 2X_{i+1} + X_{i+2}$. Triads which lead to a β_i-value greater than a fixed limit are rejected under the assumption that they cannot represent a segment of an electron track of interest. After all possible triads have been examined, the unmatched points are saved and the next deck with points is found. New

triads are found and the procedure iterates. Track segments containing the most points are examined further to ascertain their inter-relationship in an attempt to form full tracks from the segments.

For a gamma ray, two basic forms occur depending on how fast the electrons separate, the "inverted Y" and the "inverted V". In the case of the "Y" configuration, the stem is considered to be two unresolved electrons and is associated with each of the two separated tracks. Some events appear to contain only a single track segment. These are classified as either low energy electrons, or an unresolved pair (high energy, straight track), depending on the amount of Coulomb scattering. Experience has shown that the single tracks do indeed fall in these two groups with essentially no tracks having intermediate Coulomb scattering values.

There remain some spark chamber events which the computer is unable to handle satisfactorily. The following are examples of situations which cause the program to abandon an event:

1) Less than $\sim$ 45% of the total X or Y points being contained in the two longest segments,
2) Less than 13 decks containing points,
3) No acceptable triads,
4) No acceptable tracks ($\geq$ 5 points),
5) Too many segments ($\geq$ 15), which cannot be formed into longer tracks,
6) Ambiguous relationship between the two main tracks,
7) Two main tracks not joined.

Events which are abandoned by the computer are then subjected to visual analysis in the following manner. The digitized "picture" of each of these events is displayed on an automatic graphics display unit where the necessary editing is accomplished by light pen interaction and the remainder of the analysis is completed by machine, if it is an acceptable event. If it is evaluated to be a false event, it is rejected.

Although most of the results presented here are from the computer-analyzed data, extensive checks have been made by reanalyzing samples of the data visually. In its present stage of development, the computer analysis produces results of comparable or even slightly superior quality, when it is applied to high quality data. When the spark chamber efficiency is less than optimal, the computer analysis is less dependable particularly for gamma-ray energies below about 70 MeV, where the electrons undergo considerable scattering. For that reason, all of the results presented here for gamma-ray energies below 100 MeV are based on either visual analysis of the events or computer analysis checked by visual examination of the pictures.

IV. THEORETICAL BACKGROUND AND RESULTS

a) The Galactic Center Region

It is well known that mesons are produced in the interaction of cosmic rays with interstellar matter, and by far the most common mesons are π-mesons, both charged and neutral. The π° decays into two γ-rays, each with about 70 MeV in the rest frame. Many of the other mesons and hyperons also decay into neutral π mesons. As a result, the great

majority of the high energy gamma rays resulting from nuclear interaction are from π° mesons, most of which are formed in the initial interaction.

The energy spectrum of the gamma rays resulting from π° decay is quite different from that resulting from most of the other astrophysical processes, such as bremsstrahlung, synchrotron radiation, and the inverse Compton effect. The basis for the relatively unique spectrum is the π°'s isotropic decay into two gamma rays of equal energy ($\sim$ 70 MeV) in the rest frame. As a result for a given velocity of the parent π°, the probability of observing a given energy for the secondary gamma ray is a constant from a minimum energy of $W_o[(1-\beta)/(1+\beta)]^{1/2}$ to a maximum energy of $W_o[(1+\beta)/(1-\beta)]^{1/2}$ where W_o is the energy of the gamma ray in the rest frame. Thus, if the observed gamma rays come from π°'s formed by cosmic rays interacting with interstellar matter, a spectrum will be formed which peaks at W_o since this energy is always included, and extends further on the high energy side. The exact shape of the spectrum depends on the energy distribution of the cosmic rays and the details of the interaction process; the related calculations have been completed in detail in the literature, e.g. Stecker (1971). The actual intensity of the gamma rays was also calculated with the most uncertain parameters being the density of hydrogen and the cosmic ray intensity.

The OSO-III satellite experiment of Clark, Garmire, and Kraushaar (1968) and Garmire (1970) has detected a celestial gamma ray flux concentrated in the galactic plane. Their angular resolution ($\pm$15°) is

substantially larger than the structure of the plane; so the detailed structure cannot be seen. It is possible to quote the result as a line intensity and compare it to the result deduced from the 21 cm data integrated over the appropriate solid angle. The value of the galactic line intensity averaged over the observing angle of the OSO-III experiment is in the range (2 to 4) x 10^{-5} γ's/cm^2 rad sec) in reasonable agreement with expectation except near the galactic center. The intensity from the direction of the galactic center is not immediately explained. Even after normalizing to the rest of the galactic plane, the intensity averaged over a 60° wide region including the galactic center is about three times the expected flux. Kniffen and Fichtel (1970) in a preliminary letter have confirmed the existence and intensity of the flux from the galactic center with a balloon flight.

The explanation of the enhanced gamma radiation might be postulated to be due to an increase in the intensity of the cosmic radiation and interstellar matter near the center of the galaxy, or it may be due in part to interactions of electrons with matter, magnetic fields, or photons. The unique energy spectrum of the π° decay makes it possible to separate this mechanism from bremsstrahlung, synchrotron radiation, and Compton radiation all of which reflect the presumed power law spectrum of the parent electrons. Specifically, if the parent electrons have a spectrum of the form $j_e = CW^{-\alpha}$, the gamma ray spectrum will have the form $j_\gamma \propto W^{-\alpha}$ for bremsstrahlung radiation and $j_\gamma \sim W^{-(\alpha+1)/2}$, for Compton and synchrotron radiation.

The radiation observed from the galactic center and reported previously (Kniffen and Fichtel, 1970) has now been analyzed fully, including

information on the energy spectrum. Fig. 2 shows the ratio of the observed intensity to the intensity expected for atmospheric background as a function of galactic latitude for intervals of galactic longitudes from -25° to +20°. The atmospheric background normalization was determined from regions away from the galactic plane in the same flight and was found to agree to within better than 5% with that determined previously with a similar, but smaller gamma ray telescope (Fichtel et al., 1969). The excess of gamma rays above atmospheric background was determined for the interval $-6° \leq b^{II} \leq +6°$ and $-35° \leq b^{II} \leq +25°$ for the energy intervals 50 to 100 MeV and > 100 MeV. In this solid angle, there were 274 gamma rays whose measured energies were above 100 MeV compared to 210 expected from atmospheric background. Thus, the excess for gamma rays above 100 MeV corresponds to over four standard deviations and leads to a line intensity of $(2.0 \pm 0.6) \times 10^{-4}$ γ's/(cm^2·rad · sec.). The value is in good agreement with the corrected line intensity of $(1.2 \pm 0.3) \times 10^{-4}$ photons (cm^2 rad sec)$^{-1}$ for energies above 100 MeV observed by Clark, Garmire, and Kraushaar (Garmire, 1970). Both of these results are inconsistent with the upper limits (95 percent confidence) set by Frye, Staib, Zych, Hopper, Rawlinson, and Thomas (1969) for energies above 50 MeV of 3×10^{-5} (cm^2 rad sec)$^{-1}$ for a region bounded by $-2° \leq b^{II} \leq 2.3°$ and 7×10^{-5} (cm^2 rad sec)$^{-1}$ for a region bounded by $-15° \leq b^{II} \leq 15°$. The l^{II} range is similar to that of this experiment.

There is no statistically significant excess in the 50 to 100 MeV interval and the following 95% confidence upper limit was obtained:

$$R = [J(50\text{-}100 \text{ MeV})/J(> 100 \text{ MeV})] < 0.50$$

For π° decay alone, this ratio is expected to be 0.12 (Stecker, 1971) consistent with the experimental result. Current estimates of the cosmic ray electron spectra in the high energy region which would produce these gamma rays indicate that the spectral index for the electrons is between 2.5 and 2.8 (Anand et al., 1970; Agrinier et al., 1970; Bleeker et al., 1970; Earl et al., 1970; Fanselow et al., 1969; Marar et al., 1970; Nishimura et al., 1970; and Rockstroh and Webber, 1969). For an electron spectrum with $\alpha = 2.6$, the ratio R would be 2.03 for bremsstrahlung radiation and 0.74 for Compton or synchrotron radiation. The experimental result, therefore, suggests that the radiation from the galactic center region is probably predominantly from π° decay. More quantitatively, there is only a 6% chance that Compton or synchrotron radiation from electrons with a spectrum having a 2.6 exponent could make as much as a 50% contribution to the gamma radiation in this energy range and the data are in agreement with the radiation being entirely of π° decay origin.

B) Virgo

One of the most surprising results of X-ray astronomy has been the discovery (Byram et al., 1966; Friedman and Byram, 1967; Bradt et al., 1967) of a surprisingly intense extragalactic discrete source of 1 to 10 keV X-rays in the direction of the Virgo cluster. Recent high resolution satellite studies (Kellogg et al., 1971) have provided convincing evidence that the source coincides with the radio galaxy M-87 (Virgo A) and that M-84 and the quasar 3C273 are other likely discrete source emitters in the direction of Virgo. Measurements of high energy (40-100 keV) X-rays

from Virgo A have also been reported (Haymes et al., 1968; Fishman et al., 1970), but these measurements lack independent verification and, in fact, conflicting results have been reported (Peterson, 1970; McClintock et al., 1969; Webber and Reinert, 1970). Felton (1970) has summarized the existing observations over the entire electromagnetic spectrum of the "jet" of Virgo and finds that the data over 13 decades of energy are reasonably consistent with a single power law spectrum given by

$$N(E) = 8.2 \times 10^{-4} E^{-1.75} \text{ photons}/(\text{cm}^2 \text{ sec MeV}).$$

Extending this spectrum 2 to 3 decades above the highest observed energies gives an expected flux above 30 MeV of about 9×10^{-5} (cm^2 sec).

It is most probable that the power law in the visible and radio portions of the spectrum is generated by the synchrotron emission of energetic electrons traveling the magnetic fields in the source galaxy. However, until the X-ray spectrum is better known, it is not clear if this emission represents an extension of the power law synchrotrom emission at lower frequencies, which would create a very puzzling dilemma because of the very short lifetimes of the electrons at these energies, or indicates the presence of additional processes such as the thermal bremsstrahlung suggested by Sartori and Morrison (1967). The resolution of this question depends upon further experimental results, and for this reason we undertook a balloon flight to examine the Virgo region for the emission of > 30 MeV gamma radiation.

The detector was flown October 14, 1970 on a 27 million cubic foot balloon from Palestine, Texas. It reached a depth in the atmosphere of

2.5 g/cm^2 at 8:55 a.m. CDT and remained at float until terminated by command at 5:00 p.m. CDT. The detector was tilted 20° and oriented to point toward the south in order to more efficiently examine M-87 which lies at a declination which passes the meridian plane about 20° south of the Palestine latitude. M-87 passed overhead at about 12:15 p.m. CDT. At about 2:15 p.m. the detector was commanded level and allowed to examine the sky centered at a declination of about +31.5° corresponding to the latitude of the balloon.

The data from this flight were analyzed by the automatic analysis program, with no human interaction. Since a significant portion of the events below about 70 MeV require human interpretation, the analysis reported here includes only gamma rays with measured energies in excess of 100 MeV.

The background was determined by analyzing all portions of the sky which were examined except for the areas surrounding possible sources. Table I summarizes the results obtained from M-87 and 3C273. The 95 percent confidence limits were obtained by the method outlined by Fichtel et al. (1969). The M-87 limit clearly rules out the possibility that the power law spectrum extends unaltered to gamma ray energies as seen in Fig. 3. However, the limit places no constraint on the secondary production model of Felten (1968) which attempts to explain the presence of electrons in the jet as arising from the decay of pions produced in collisions of energetic protons from the core with matter in the jet. The decay of accompanying neutral pions would be expected to produce a gamma ray flux orders of magnitude below the observed limit.

C) Crab Nebula

On July 15, 1969, a balloon flight of the 50 cm by 50 cm spark chamber was conducted at Palestine, Texas, to examine the Crab nebula for possible discrete source gamma ray emission, either steady or pulsed. Unfortunately a random electronic component failure prevented a full exposure to this region. No evidence was obtained for discrete source gamma ray emission in the Crab nebula and 95 percent confidence limits of $6 \times 10^{-5}/(cm^2\ sec^1)$ and $8 \times 10^{-5}/(cm^2\ sec^1)$ were obtained for integral fluxes above 50 and 100 MeV, respectively. The arrival times of the gamma rays coming from the direction of the Crab nebula were tested against the observed optical period for this date (Fazio and Helmken, 1971) and no evidence for pulsation was seen. The limited statistics prevent the upper limit for the pulsed mode from being substantially lower than those for the steady mode given above.

ACKNOWLEDGMENTS

We wish to express our appreciation to S. Derdeyn, C. Ehrmann, A. Mascaro, R. Ross, and R. Smith for their outstanding engineering support and to R. Marsh for her long hours of careful work in support of the data analysis. Also, we acknowledge the stimulating discussions that we had with H. Ogelman during the early phases of the experiment. For the three successful flights, we are indebted to the balloon-launching crews of the Australian Department of Supply at Mildura, Victoria, and the NCAR at Palestine, Texas, and to the personnel of the Office of Naval Research.

REFERENCES

Anand, K.C., Daniel, R.R., and Stephens, S.A., 1970, Acta Physica Supp. to Vol. 29, 1, 229.

Agrinier, B., Koechlin, Y., Parlier, B., Paul, J., Vasseur, T., Boella, G., Sironi, G., Russo, A., and Scarsi, L., 1970, Acta Physica Supp. to Vol. 29, 1, 203.

Bleeker, J.A.M., Burger, J.J., Deerenberg, A.J.M., Van De Hulst, H.C., Scheepmaker, A., Swanenburg, B.N., and Tanaka, Y., 1970, Acta Physica Suppl. to Vol. 29, 1, 217.

Bradt, H., Mayer, W., Naranan, S., Rappaport, S., and Spada, G., 1967, Ap. J. 150, L199, 1967.

Byram, E. T., Chubb, T. A., and Friedman, H., 1966, Science 152, 66.

Clark, G.W., Garmire, G.P., and Kraushaar, W.L., 1968, Ap. J. (Letters), 153, L203.

Earl, J.A., Neely, D.E., and Rygg, T.A., 1970, U. of Md. Technical Report 70-076.

Fanselow, J.L., Hartman, R.C., Hildebrand, R.H., and Meyer, P., 1969, Ap. J. 158, 771.

Fazio, G., and Helmken, H., 1971, Smithsonian Institution Astrophysical Observatory Computer Programs, private communication.

Felten, J.E., 1968, Ap. J. 151, 861.

Felten, J.E., 1970, I.A.U. Symposium No. 37, Non-Solar X- and Gamma-Ray Astronomy, L. Gratton (ed.), D. Reidel (Dordrecht), p. 216.

Fichtel, C.E., Kniffen, D.A., and Ogelman, H.B., 1969, Ap. J. 158, 193.

Fishman, G.J., Harnden, F.R., Jr., and Haymes, R.C., 1970, I.A.U. Symposium No. 37, Non-Solar X- and Gamma-Ray Astronomy, L. Gratton (ed.), D. Reidel (Dordrecht), p. 116.

Friedman, H. and Byram, E.T., 1967, Science 158, 257.

Frye, G.M., Staib, J.A., Zych, A.D., Hopper, V.D., Rawlinson, W.R., and Thomas, J.A., 1969, Nature 223, 1320.

Garmire, G.P., 1970, Bull. Am. Phys. Soc., 15, 564.

Haymes, R.C., Ellis, D.V., Fishman, G.J., Kurfess, J.D., and Tucker, W.H., 1968, Ap. J. 151, L131.

Kellog, E., Gursky, H., Leong, C., Schreier, E., Tananbaum, H., and Giacconi, R., 1971, Ap. J. (Letters) 165, L49.

Kniffen, D.A., and Fichtel, C.E., 1970, Ap. J. (Letters) 161, L157.

Marar, T.M.K., Freier, P.S., and Waddington, C.J., 1970, Acta Physica Suppl. to Vol. 29, 1, 137.

McClintock, J.E., Lewin, W.H.G., Sullivan, R.J. and Clark, G.W., 1969, Nature 223, 162.

Nishimura, J., Mikumo, E., Mito, I., Niu, K., Ohta, I. and Taira, 1970, Acta Physica Suppl. to Vol. 29, 1, 239.

Peterson, L.E., 1970, I.A.U. Symposium No. 37, Non-Solar X- and Gamma-Ray Astronomy, L. Gratton (ed.), D. Reidel (Dordrecht), p. 59.

Ross, R., Ehrmann, C., Fichtel, C., Kniffen, D., and Ogelman, H., 1969, IEEE Transactions on Nuclear Science, NS-16, 127.

Rockstroh, J. and Webber, W.R., 1969, J. Geophys. Res. 74, 5041.

Sartori, L. and Morrison, P., 1967, Ap. J. 150, 385.

Stecker, F.W., 1971, Cosmic Gamma Rays, NASA SP-249, U. S. Government Printing Office.

Webber, W. R. and Reinert, C.P., 1970, Ap. J. 162, 833.

FIGURE CAPTIONS

Fig. 1: Schematic diagram of the 0.5m x 0.5m digitized spark-chamber γ-ray telescope.

Fig. 2: Ratio of observed line intensity of > 100 MeV gamma rays to expected background intensity for $-25° \leq \ell^{II} \leq +20°$, plotted as a function of galactic latitude, b^{II}. The lower curve shows data plotted in 2° bin widths, the approximate angular resolution of the detector. The upper curve includes the same data in $\pm 6°$ bins to increase statistics and more clearly show the latitudinal dependence.

Fig. 3: The upper limit to > 100 MeV gamma rays from M-87 obtained in this experiment is plotted together with the empirical curve for the jet in M-87 obtained by Felten (1970). The dashed curve represents an extrapolation of the curve above the highest observed energies.

TABLE I. DATA SUMMARY FOR POSSIBLE DISCRETE SOURCES IN THE DIRECTION OF M87 AND 3C 273

GAMMA RAY LIMITS
$E\gamma \geq 100$ MeV

	M87	3C273
NUMBER OF GAMMAS EXPECTED (3° x 3°)	7.4	5.0
NUMBER OF GAMMAS OBSERVED	8.0	3.0
95 % CONFIDENCE NUMBER LIMIT	7.8	4.8
95 % CONFIDENCE FLUX LIMIT (10^{-5}/CM SEC)	1.0	1.0

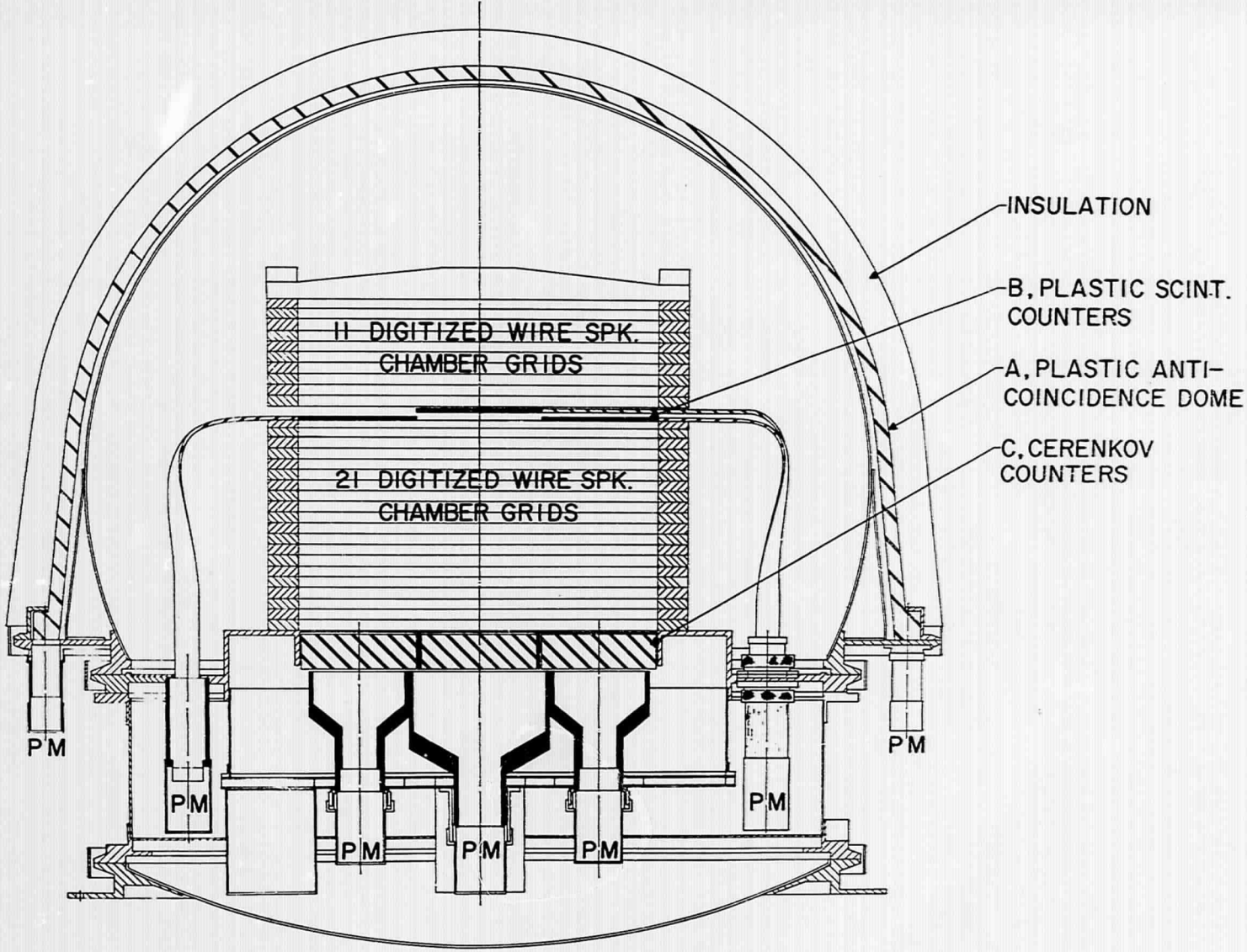

SCHEMATIC OF 1/2 x 1/2 M. DIGITIZED SPARK CHAMBER GAMMA RAY TELESCOPE

FIG. 1

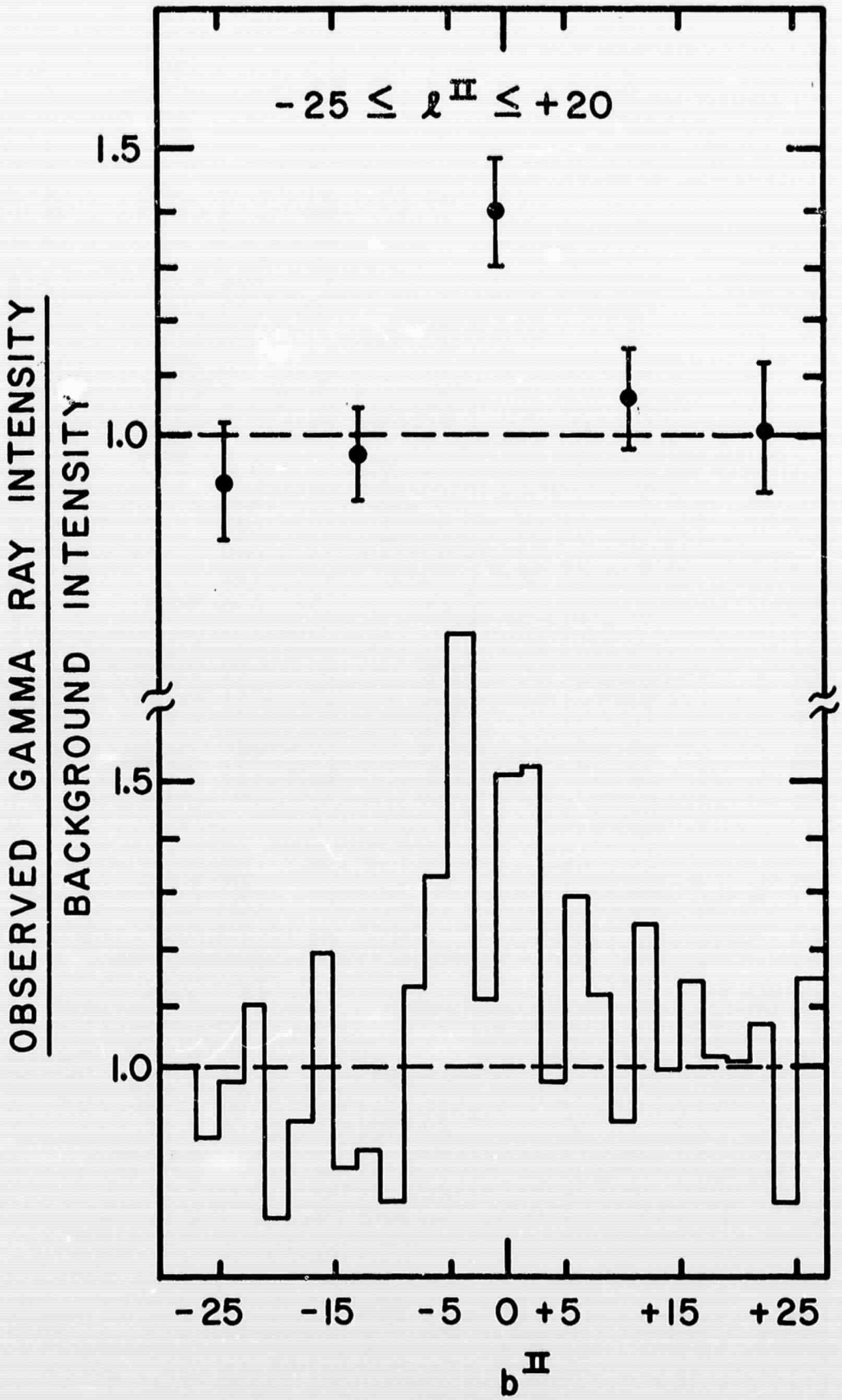
$-25 \leq \ell^{II} \leq +20$
OBSERVED GAMMA RAY INTENSITY
BACKGROUND INTENSITY
1.5
1.0
1.5
1.0
-25
-15
-5
0
+5
+15
+25
b^{II}

FIG. 2

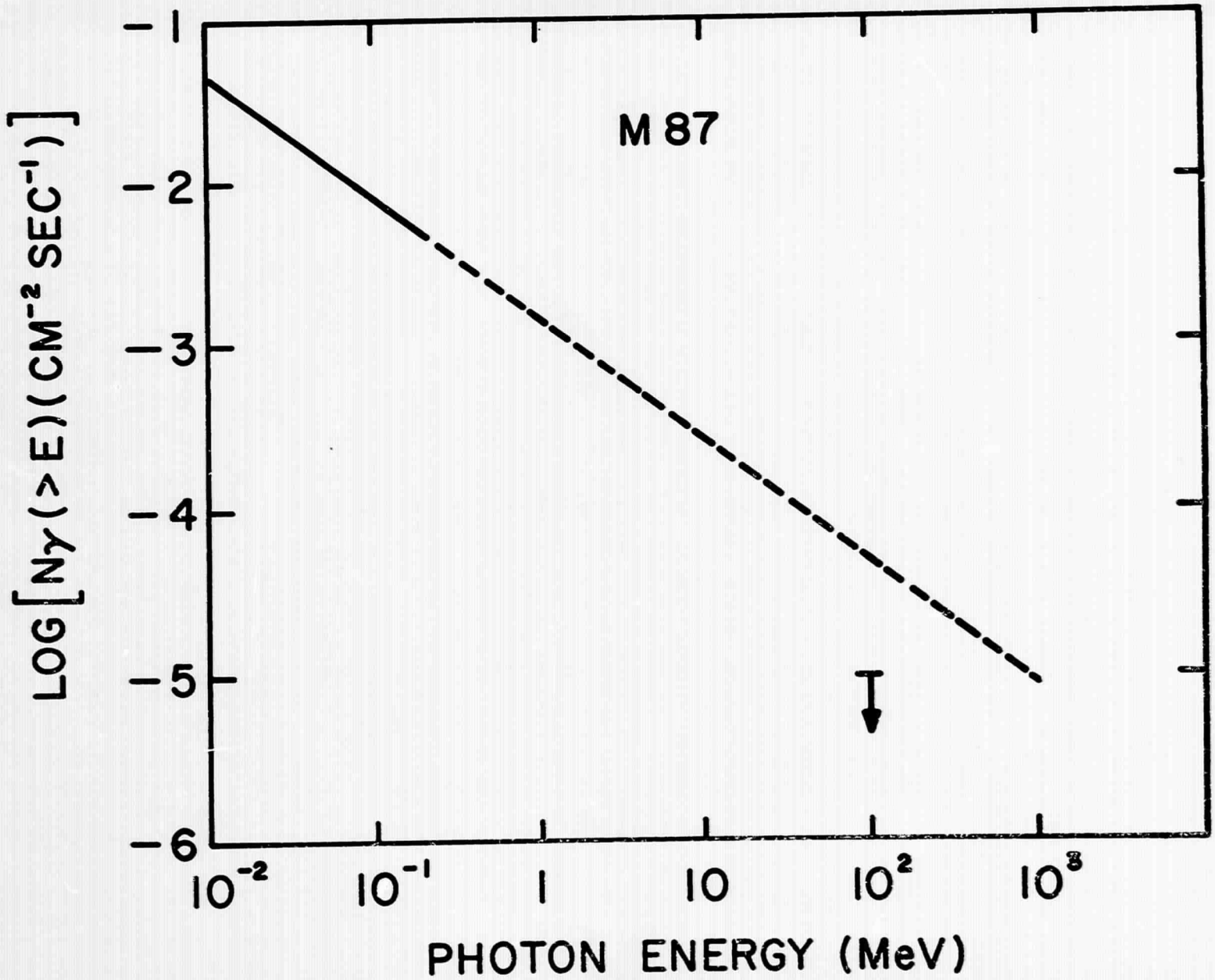
M 87
LOG [Nγ (>E) (CM⁻² SEC⁻¹)]
-1
-2
-3
-4
-5
-6
10⁻²
10⁻¹
1
10
10²
10³
PHOTON ENERGY (MeV)
FIG. 3